# Thermal rectification in a double quantum dots system with a polaron effect

Gaomin Tang,[1,2] Lei Zhang,[1,3,4,*] and Jian Wang[1,†]

[1]*Department of Physics and the Center of Theoretical and Computational Physics, The University of Hong Kong, Hong Kong, China*
[2]*Department of Physics, National University of Singapore, Singapore 117551, Republic of Singapore*
[3]*State Key Laboratory of Quantum Optics and Quantum Optics Devices, Institute of Laser Spectroscopy,*
*Shanxi University, Taiyuan 030006, China*
[4]*Collaborative Innovation Center of Extreme Optics, Shanxi University, Taiyuan 030006, China*

We investigate the rectification of heat current carried by electrons through a double quantum dot (DQD) system under a temperature bias. The DQD can be realized by molecules such as suspended carbon nanotubes and be described by the Anderson-Holstein model in the presence of electron-phonon interaction. Strong electron-phonon interaction can lead to formation of polaronic states in which electronic states are dressed by a phonon cloud. Dressed tunneling approximation (DTA), which is nonperturbative in dealing with strong electron-phonon interaction, is employed to obtain the heat current expression. In DTA, self-energies are dressed by a phonon cloud operator and are temperature dependent. The temperature dependency of the imaginary part of the dressed retarded self-energy gives rise to the asymmetry of the system and is the necessary condition of thermal rectification. On top of this, one can either tune DQD effective energy levels such that $|\bar{\epsilon}_1| \neq |\bar{\epsilon}_2|$ or have asymmetric dot-lead couplings to achieve thermal rectification. We numerically find that increasing electron-phonon coupling and reducing interdot coupling can improve the thermal rectification effect, while the electronic heat current is reduced.

## I. INTRODUCTION

Understanding and controlling heat flow become essential for a variety of applications in heating, refrigeration, heat-assist information storage, and energy conversion in modern times [1–3]. In analogy to electric diodes as the primary building block in the electronics industry, a thermal diode or rectifier becomes crucial in managing heat flow by changing heat current magnitude with the reversal of temperature bias. Thermal rectification has been reported in various systems such as semiconductor quantum dot junction [4], magnonic junction [5], spin Seebeck engine [6,7], topological insulator-superconductor junction [8], normal metal-superconductor junction [9–11], near-field radiative heat transfer [12], geometric asymmetric structures [13–16], etc. Heat current can be transferred via different types of energy carriers [17,18], such as magnons [5–7], electrons [8–11,19–24], photons [12,25], phonons [26,27], acoustic wave [28,29], etc.. Regardless of the type of junctions and energy carriers, the key ingredient required for achieving thermal rectification is structural asymmetry [30].

Over the past decades, rapid experimental development of nanotechnology enables us to fabricate the single-molecule junctions [31–33]. The elastic mechanical deformation caused by charging of the molecule can give rise to electron-phonon interaction. A single-molecule junction could be modeled and measured as a quantum dot or serial double quantum dots (DQDs) described by the Anderson-Holstein model [34,35] connected to two leads. Suspended carbon nanotubes (CNTs),

which are free to oscillate due to high $Q$ factors and stiffness, become very favorable in experiments [36]. Recently, it has been reported that the electron-phonon coupling strength of a suspended CNT can be tailored [37]. The strong electron-phonon coupling in molecular junctions can lead to the polaronic regime in which electronic states are dressed by a phonon cloud [38,39]. The polaronic effect exhibits novel transport properties, such as negative differential conductance [33,40,41], phonon-assisted current steps [41–46], Franck-Condon blockade [45–47], sign change in the shot noise correction [48], etc.. Rectification effect of electric current in a DQD system in the presence of strong polaron effect [49], by Pauli exclusion [50] or through fermionic reservoir engineering [51], has been reported. Thermal rectification in quantum dots with strong Coulomb interaction has been studied recently [22]. Thermal rectification of DQD employing electron-phonon interaction is yet to be revealed.

In this work we report the rectification effect of electronic heat current through a DQD system in a polaronic regime under a temperature bias. A nonperturbative approach, i.e., the dressed tunneling approximation (DTA) [42–44], is employed to deal with strong electron-phonon interaction. Self-energies dressed by a phonon cloud operator due to electron-phonon couplings are introduced. The expression of electronic heat current is obtained from the equation of motion technique together with DTA. We find that the necessary condition to realize the rectification effect in the DQD system is the temperature dependency of dressed retarded self-energies. In addition, one should either tune the DQD levels $\bar{\epsilon}_\nu$ satisfying $|\bar{\epsilon}_1| \neq |\bar{\epsilon}_2|$ or set the dot-lead couplings unequal to achieve thermal rectification. We show the behaviors of dressed retarded self-energy with respect to temperatures and electron-phonon coupling constant

———————
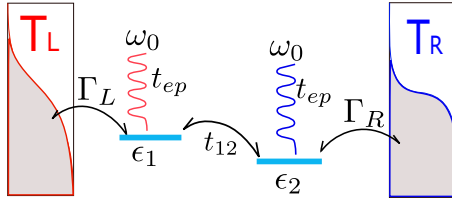*zhanglei@sxu.edu.cn
†jianwang@hku.hk

FIG. 1. Sketch of a DQD being coupled to the left and right lead with temperatures $T_L$ and $T_R$. Each quantum dot strongly interacts with a local vibrational mode, which has the same temperature with the corresponding lead. The central DQD can be described by the Anderson-Holstein model.

$g$. We find that increasing $g$ and decreasing interdot coupling can improve rectification effect, while heat current is reduced.

The rest of the article is organized as follows. In Sec. II the model Hamiltonian of the DQD molecular junction is introduced and the expression of electronic heat current is given in terms of nonequilibrium Green's function (NEGF) formalism. In Sec. III, since the temperature dependency of dressed retarded self-energy is crucial to achieve thermal rectification, we first show its behaviors with respect to different temperatures and electron-phonon coupling. Then we investigate the heat current rectification effect by changing system parameters. Finally, a brief conclusion is drawn in Sec. IV.

## II. MODEL AND THEORETICAL FORMALISM

We consider our setup as a serial DQD system made of molecules connected to its left and right lead with different temperatures (see Fig. 1). The DQD can be realized using CNT, with the central part being fixed and each lateral part suspended as the quantum dot [40]. Each quantum dot shall be close to the lead that it connects with, so that the localized vibrational mode of each quantum dot bears the same temperature with a corresponding lead. The hopping between the two quantum dots can be tuned using a gate voltage applied on the central fixed part. The central DQD can be described by the Anderson-Holstein model [34,35] and its Hamiltonian is expressed as (in natural units, $\hbar = k_B = e = m_e = 1$)

$$H_{\text{DQD}} = \sum_{\nu=1,2} [\epsilon_\nu \hat{n}_\nu + t_{ep\nu}(a_\nu^\dagger + a_\nu)\hat{n}_\nu + \omega_0 a_\nu^\dagger a_\nu]$$
$$+ t_{12}(d_1^\dagger d_2 + d_2^\dagger d_1). \qquad (1)$$

Here $\epsilon_\nu$ is the bare electronic energy level of the site $\nu$ quantum dot, $\omega_0$ is the frequency of the localized phonon, $d_\nu^\dagger$ ($a_\nu^\dagger$) denotes the electron (phonon) creation operator, and the occupation operator is $\hat{n}_\nu = d_\nu^\dagger d_\nu$. $t_{12}$ is the interdot hopping amplitude. We assume that electron-phonon couplings in DQD are the same constant with $t_{ep1} = t_{ep2} = t_{ep}$. The total Hamiltonian reads as

$$H = H_{\text{DQD}} + \sum_\alpha H_\alpha + H_T, \qquad (2)$$

with the Hamiltonians of the leads

$$H_\alpha = \sum_{k,\alpha} \epsilon_{k\alpha} c_{k\alpha}^\dagger c_{k\alpha}, \qquad (3)$$

where $c_{k\alpha}^\dagger$ creates an electron in lead $\alpha$ and the tunneling Hamiltonian between the dots and the leads,

$$H_T = \sum_k (t_{kL} c_{kL}^\dagger d_1 + t_{kR} c_{kR}^\dagger d_2 + \text{H.c.}). \qquad (4)$$

The indices $k\alpha = kL, kR$ are used to label the different states in the left and right leads, and $t_{k\alpha}$ is the tunneling amplitude between quantum dot and state $k$ in lead $\alpha$. The tunneling rates of both leads are assumed to be independent of energy (wide band limit) as

$$\Gamma_\alpha(\omega) = \text{Im} \sum_k \frac{|t_{k\alpha}|^2}{\omega - \epsilon_{k\alpha} - i0^+} = \Gamma_\alpha, \qquad (5)$$

and one can denote $\Gamma = \Gamma_L + \Gamma_R$. The DQD model here is similar to the disordered molecular nanowire whose transport properties has been studied [24]. The leads chemical potentials here are both set to zero $\mu_L = \mu_R = 0$, and a temperature bias is applied at two leads with $\Delta T = T_L - T_R$ to induce electronic transport.

Applying the Lang-Firsov unitary transformation [24,52] given by

$$\bar{H} = SHS^\dagger, \quad S = \exp\left[g \sum_\nu \hat{n}_\nu (a_\nu^\dagger - a_\nu)\right], \quad g = \frac{t_{ep}}{\omega_0}, \qquad (6)$$

one can eliminate the electron-phonon coupling term, and get the central DQD Hamiltonian as

$$\bar{H}_{\text{DQD}} = \sum_{\nu=1,2} [\bar{\epsilon}_\nu \hat{n}_\nu + \omega_0 a_\nu^\dagger a_\nu] + t_{12}(d_1^\dagger d_2 + d_2^\dagger d_1), \qquad (7)$$

where the effective bare QD electronic energies are changed to be $\bar{\epsilon}_\nu = \epsilon_\nu - g^2 \omega_0$. Throughout this work, the effective bare QD electron energies are termed as QD electron energies for convenience. The tunneling Hamiltonian is transformed to be

$$\bar{H}_T = \sum_k (t_{kL} c_{kL}^\dagger X_1 d_1 + t_{kR} c_{kR}^\dagger X_2 d_2 + \text{H.c.}), \qquad (8)$$

with the phonon cloud operator $X_\nu = \exp[g(a_\nu - a_\nu^\dagger)]$, while the Hamiltonian of the uncoupled leads remains unchanged. The energy current carried by electrons through lead $\alpha$ is defined as the time evolution of the Hamiltonian of lead $\alpha$ with the form [53,54] $I_\alpha^E = -\langle \dot{\hat{H}}_\alpha \rangle = -i \langle [\hat{H}_\alpha, \bar{H}] \rangle$. Since no voltage bias is applied, the energy current is the same as the heat current, and the electronic heat current through the left lead reads as

$$I_h = \sum_k [i\epsilon_{kL} t_{kL} \langle c_{kL}^\dagger(t) X_1(t) d_1(t) \rangle + \text{H.c.}]. \qquad (9)$$

Detailed derivations of heat current formula and Dyson equation in the time domain under the dressed tunneling approximation (DTA) are shown in the Appendix.

The DQD Green's function on the Keldysh contour is defined as [55]

$$G_{\nu\nu'}(\tau_1, \tau_2) = -i\langle \mathcal{T}_C d_{\nu'}^\dagger(\tau_2) d_\nu(\tau_1) \rangle, \qquad (10)$$

with $\nu, \nu' = 1, 2$ labeling quantum dots. By transforming Eq. (A21) to energy domain and then performing Keldysh rotation [56], the Dyson equation for the retarded Green's

function in the energy domain bears the form

$$\mathbf{G}^r = \mathbf{g}^r + \mathbf{g}^r\left(\Sigma_d^r + \mathbf{t}\right)\mathbf{G}^r, \tag{11}$$

where $g_\nu$ is the free DQD Green's function of site $\nu$ without coupling to the leads. The lesser and greater Green's functions are given by the following Keldysh equations:

$$\mathbf{G}^{+-} = \mathbf{G}^r \Sigma_d^{+-} \mathbf{G}^a, \tag{12}$$

$$\mathbf{G}^{-+} = \mathbf{G}^r \Sigma_d^{-+} \mathbf{G}^a. \tag{13}$$

The Green's functions and self-energies in the above equations have the structure as the following:

$$\mathbf{G} = \begin{pmatrix} G_{11} & G_{12} \\ G_{21} & G_{22} \end{pmatrix}, \quad \mathbf{g} = \begin{pmatrix} g_1 & \\ & g_2 \end{pmatrix},$$

$$\Sigma_d = \begin{pmatrix} \Sigma_{dL} & \\ & \Sigma_{dR} \end{pmatrix}, \quad \mathbf{t} = \begin{pmatrix} & t_{12} \\ t_{21} & \end{pmatrix}.$$

In the wide band limit, the dressed lesser and greater self-energies in the energy domain are given by

$$\Sigma_{d\alpha}^{+-}(\omega) = -\sum_m A_{\alpha m} i \Gamma_\alpha f_{\alpha+m}, \tag{14}$$

$$\Sigma_{d\alpha}^{-+}(\omega) = -\sum_m A_{\alpha m} i \Gamma_\alpha [f_{\alpha-m} - 1], \tag{15}$$

where

$$f_{\alpha+m} = 1/\{\exp[\beta_\alpha(\omega + m\omega_0 - \mu_\alpha)] + 1\}. \tag{16}$$

The dressed retarded self-energy in energy domain is obtained through the Fourier transformation of the time domain counterpart $\Sigma_d^r(t_1, t_2) = \theta(t_1 - t_2)[\Sigma_d^{+-}(t_1, t_2) - \Sigma_d^{-+}(t_1, t_2)]$, so that [42–44]

$$\Sigma_{d\alpha}^r(\omega) = \sum_m A_{\alpha m} \int \frac{dE}{2\pi} \frac{\Gamma_\alpha[1 - f_{\alpha-m}(E) + f_{\alpha+m}(E)]}{\omega - E + i0^+}. \tag{17}$$

The real and imaginary part of the dressed retarded self-energy can be obtained using Plemelj formula $1/(E \pm i0^+) = P(1/E) \mp i\pi\delta(E)$ which facilitates the numerical calculation as well. We can directly prove that the real part and imaginary part are odd and even function with respect to the chemical potential, respectively [42,54], with the expressions

$$\text{Re}\big[\Sigma_{d\alpha}^r(\mu_\alpha + \omega)\big] = -\text{Re}\big[\Sigma_{d\alpha}^r(\mu_\alpha - \omega)\big],$$

$$\text{Im}\big[\Sigma_{d\alpha}^r(\mu_\alpha + \omega)\big] = \text{Im}\big[\Sigma_{d\alpha}^r(\mu_\alpha - \omega)\big]. \tag{18}$$

Since the chemical potential of both leads are set to zero, the real and imaginary part of the dressed retarded self-energy are even and odd functions of energy.

The current expression in the energy domain can be obtained by Fourier transforming from the time domain expression Eq. (A5), it is in a Meir-Wingreen form [55] with dressed self-energy The current expression could be expressed by an integral in the energy domain as

$$I_h = \int \frac{d\omega}{2\pi} \hbar\omega[G_{11}^{+-}(\omega)\Sigma_{dL}^{-+}(\omega) - G_{11}^{-+}(\omega)\Sigma_{dL}^{+-}(\omega)] = \int \frac{d\omega}{2\pi} \hbar\omega|G_{12}^r(\omega)|^2[\Sigma_{dL}^{-+}(\omega)\Sigma_{dR}^{+-}(\omega) - \Sigma_{dL}^{+-}(\omega)\Sigma_{dR}^{-+}(\omega)]. \tag{19}$$

Further simplification enables us to arrive at the heat current expression

$$I_h = \int \frac{d\omega}{2\pi} \hbar\omega T(\omega) \sum_{mn} A_{Lm} A_{Rn}[f_{L+m}(1 - f_{R-n}) - f_{R+n}(1 - f_{L-m})]. \tag{20}$$

In this expression $T(\omega)$ is the transmission coefficient with the form

$$T(\omega) = \big|G_{12}^r(\omega)\big|^2 \Gamma_L \Gamma_R. \tag{21}$$

The expression of $G_{12}^r(\omega)$ is obtained from Eq. (11),

$$G_{12}^r(\omega) = \frac{t_{12}}{[\omega - \bar{\epsilon}_1 - \Sigma_{dL}^r(\omega)][\omega - \bar{\epsilon}_2 - \Sigma_{dR}^r(\omega)] - t_{12}^2}. \tag{22}$$

We can see that the DTA provides a clear physical picture for phonon-assisted electronic heat flow. An electron coming from the left lead with energy $\omega$ absorbs (emits) $m > 0$ ($m < 0$) vibrational quanta and tunnels into the DQD, and then flows into the right lead by emitting (absorbing) $n < 0$ ($n > 0$) vibrational quanta.

Now we discuss the thermal rectification effect under temperature reversal $T_L \leftrightarrow T_R$. we let $Y(\omega) = f_{L+m}(\omega)[1 - f_{R-n}(\omega)] - f_{R+n}(\omega)[1 - f_{L-m}(\omega)]$, and denote tildes above $Y(\omega)$ and $G_{12}^r(\omega)$ to be $\widetilde{Y}(\omega)$ and $\widetilde{G}_{12}^r(\omega)$ to be the corresponding quantities after temperature reversal. One can verify the relation $Y(\omega) = -\widetilde{Y}(\omega) = \widetilde{Y}(-\omega)$ where the equality $Y(\omega) =$

$\widetilde{Y}(-\omega)$ is proved using $\sum_m A_{\alpha m} f_{\alpha+m}(\omega) = \sum_n A_{\alpha n}[1 - f_{\alpha-n}(-\omega)]$. If the dressed retarded self-energy $\Sigma_{d\alpha}^r(\omega)$ is temperature independent, one can easily see that $G_{12}^r(\omega)$ in Eq. (22) does not change with respect to temperature reversal so that heat current is symmetric under temperature reversal. Hence the temperature dependency of dressed self-energy is the necessary condition for thermal rectification. However, it is not a sufficient condition. If the junction has a symmetric coupling $\Gamma_L = \Gamma_R$, $G_{12}^r(\omega) = \widetilde{G}_{12}^r(\omega)$ holds for $\bar{\epsilon}_1 = \bar{\epsilon}_2$, and $|G_{12}^r(\omega)| = |\widetilde{G}_{12}^r(-\omega)|$ holds for $\bar{\epsilon}_1 = \pm\bar{\epsilon}_2$. The later is proved using parity of $\Sigma_{d\alpha}^r$ shown in Eq. (18). To conclude, in order to have thermal rectification in the DQD system with temperature dependent self-energies, one should either have asymmetric dot-lead coupling $\Gamma_L \neq \Gamma_R$ or tune the effective DQD levels such that $|\bar{\epsilon}_1| \neq |\bar{\epsilon}_2|$.

## III. NUMERICAL RESULTS

In this section we will first present the numerical calculation of the behaviors of dressed retarded self-energy with respect to temperature and electron-phonon coupling constant $g$, and then we will verify the conditions of achieving thermal rectification
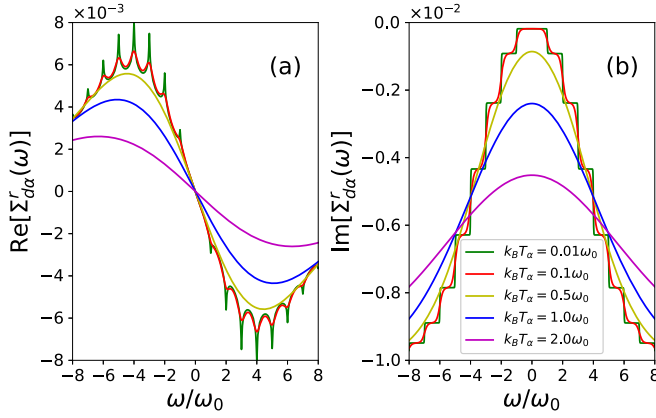
FIG. 2. Real and imaginary part of dressed retarded self-energies at different temperatures. Coupling constant is chosen as $g = 2.0$.

and examine the rectification effect by varying parameters. We assume weak coupling strengths between DQD and two leads with $\Gamma = 0.2\omega_0$ during the numerical calculations.

### A. Dressed retarded self-energy

In Fig. 2 we plot the real and imaginary part of dressed retarded self-energies $\Sigma^r_{d\alpha}$ at different temperatures with coupling constant $g = 2.0$. We can see that the real part and imaginary part are odd and even functions of energy, respectively. The real part of the dressed retarded self-energy shows peaks with logarithmic singularities at $n\omega_0$ [42]. With increasing of temperature, these peaks become small in magnitude and eventually vanish. Meanwhile, the magnitude of both real and imaginary parts decrease as well. The imaginary part has stepwise structures at low temperatures due to the opening of the inelastic channels. The stepwise structures get smoothed and vanishes at high temperatures with increasing temperatures.

The real and imaginary parts of $\Sigma^r_{d\alpha}$ at different $g$ are shown in Fig. 3 ($k_B T_\alpha = 0.2\omega_0$ for upper panels and $k_B T_\alpha = 2.0\omega_0$ for lower panels). With increasing of the electron-phonon coupling constant $g$, the magnitude of the real part increases, and the maximal (or minimal) point shift towards smaller (larger) $\omega$. The imaginary part is always negative and increases with increasing $g$ in the whole range of $\omega$ shown.

### B. Thermal rectification

In this subsection we plot electronic heat currents $I_h$ versus $\Delta T / (2T_0)$ with $\Delta T = T_L - T_R$ and $k_B T_0 = (T_L + T_R)/2 = 1.5\omega_0$ to test the condition of realizing thermal rectification. A thermal rectification ratio in this work is defined as

$$R_h = \frac{\max(|I_h(\Delta T > 0)|, |I_h(\Delta T < 0)|)}{\min(|I_h(\Delta T > 0)|, |I_h(\Delta T < 0)|)} - 1. \quad (23)$$

Heat currents versus $\Delta T / (2T_0)$ by varying effective DQD levels $\bar{\epsilon}_\nu$ and dot-lead couplings $\Gamma_\alpha$ are shown in Fig. 4 for the following three cases: (i) $\bar{\epsilon}_1 = -\bar{\epsilon}_2 = 0.3\omega_0$ with $\Gamma_L = \Gamma_R$; (ii) $\bar{\epsilon}_1 = 0$ and $\bar{\epsilon}_2 = -0.6\omega_0$ with $\Gamma_L = \Gamma_R$; and (iii) $\bar{\epsilon}_1 = \bar{\epsilon}_2 = 0$ with $\Gamma_L = 0.25\Gamma_R$. The corresponding rectification ratios are
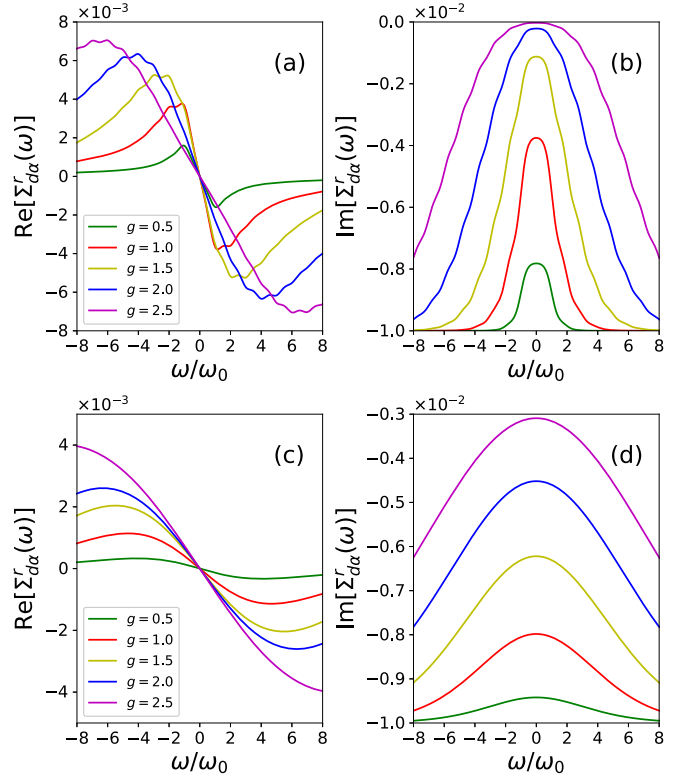


FIG. 3. Real and imaginary part of dressed retarded self-energies at different $g$. $k_B T_\alpha = 0.2\omega_0$ for upper panels and $k_B T_\alpha = 2.0\omega_0$ for lower panels.

plotted in the right panel. For the case of $\bar{\epsilon}_1 = -\bar{\epsilon}_2$ with equal dot-lead coupling, the heat current is symmetric with respect to temperature reversal with a vanished thermal rectification ratio. Thermal rectification occurs by breaking the condition $\bar{\epsilon}_1 = \pm\bar{\epsilon}_2$ [case (ii)] or in the system with unequal dot-lead couplings [case (iii)].

To further investigate the factors that affect thermal rectification, we show heat currents and their corresponding thermal
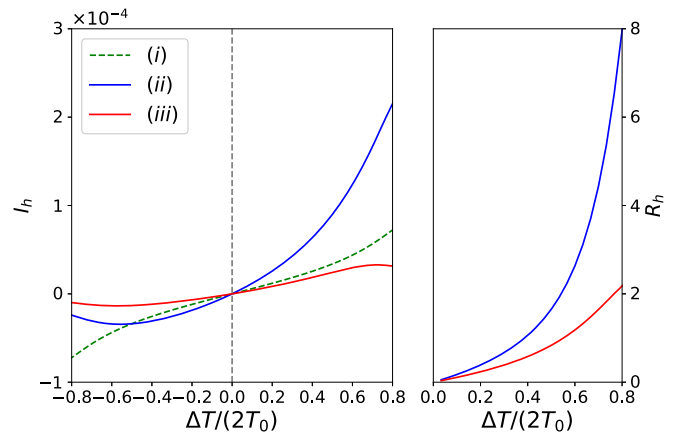


FIG. 4. Heat current $I_h$ as a function of $\Delta T / (2T_0)$ by varying $\bar{\epsilon}_\nu$ and $\Gamma_\alpha$: (i) $\bar{\epsilon}_1 = -\bar{\epsilon}_2 = 0.3\omega_0$ with $\Gamma_L = \Gamma_R$; (ii) $\bar{\epsilon}_1 = 0$ and $\bar{\epsilon}_2 = -0.6\omega_0$ with $\Gamma_L = \Gamma_R$; and (iii) $\bar{\epsilon}_1 = \bar{\epsilon}_2 = 0$ with $\Gamma_L = 0.25\Gamma_R$. Other parameters are chosen as $t_{12} = 0.1\omega_0$, $g = 2.0$. The corresponding rectification ratios are plotted in the right panel.
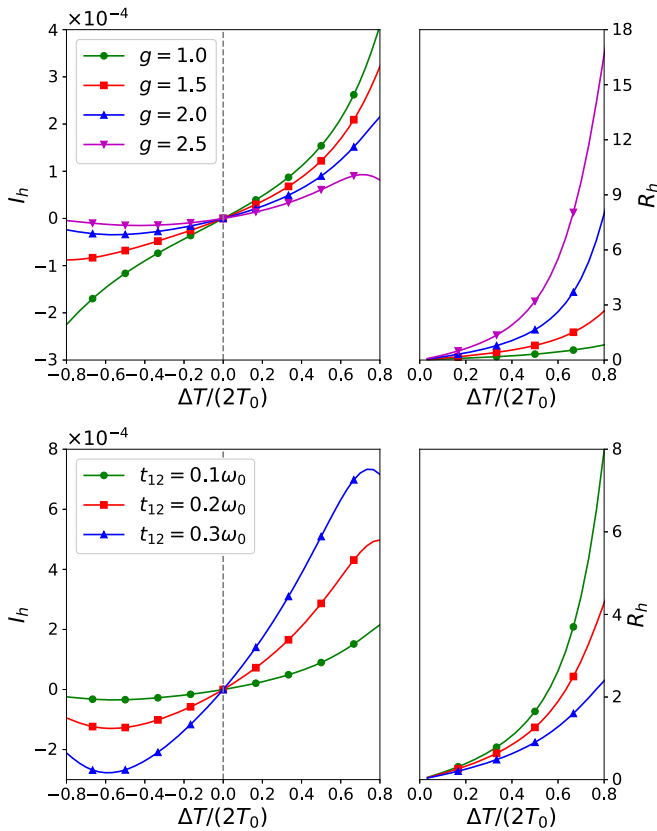
FIG. 5. Heat current and the corresponding heat rectification ratio as a function of $\Delta T/(2T_0)$ by varying coupling constant $g$ with $t_{12} = 0.1\omega_0$ (upper panels) and interdot hopping amplitude $t_{12}$ with $g = 2.0$ (lower panels).

rectification ratios for different coupling constants $g$ in the upper panels of Fig. 5 and interdot hopping amplitudes $t_{12}$ in the lower panels of Fig. 5. With increasing $g$ or decreasing $t_{12}$ we observe that the heat current amplitude decreases while the thermal rectification ratio increases. This is because electron-phonon interaction strength increases with increasing $g$ so that it becomes more difficult for the electron to escape the phonon cloud, thus reducing the thermal current amplitude. In the meantime, the nonlinearity becomes more pronounced with increasing $g$ and this is favorable to the rectification effect. Increasing interdot hopping $t_{12}$ enables the electron to tunnel across the junction more easily and reduces the influence of electron-phonon interaction, so that heat current amplitude increases and rectification ratio decreases.

## IV. CONCLUSION

In this work we have studied the rectification of electronic heat current through a double quantum dot junction under a temperature bias. The DQD in the presence of strong electron-phonon interaction is described by the Anderson-Holstein model and can lead to the formation of polaronic states in which electronic states are dressed by a phonon cloud. Dressed tunneling approximation is employed to deal with strong electron-phonon interaction by dressing the self-energies with a phonon cloud operator. The heat current expression is obtained using the equation of motion method. We found that the real and

imaginary parts of dressed retarded self-energy is, respectively, odd and even functions of energy with respect to chemical potential. The temperature dependency of dressed self-energy is due to the fact that the temperature of the vibrational mode in each dot is the same with the corresponding lead it couples. This gives rise to the asymmetry of the system and is the necessary condition of thermal rectification. On top of the temperature dependency of self-energies, one should either have asymmetric dot-lead couplings or tune DQD effective levels satisfying $|\bar{\epsilon}_1| \neq |\bar{\epsilon}_2|$ to rectify heat current.

In the numerical calculations we show the behaviors of dressed retarded self-energy with respect to temperatures and electron-phonon coupling constant $g$. With increasing temperature, the peaks at $n\omega_0$ of the real part of the dressed retarded self-energy become small in magnitude and eventually vanish. Meanwhile, the magnitude of both real and imaginary parts decrease, and the stepwise structures of the imaginary part get smoothed and vanishes at high temperatures. With increasing the electron-phonon coupling constant $g$, the maximal (or minimal) point shift towards smaller (larger) $\omega$. The imaginary part is always negative and increases with increasing $g$ in the whole range of $\omega$.

The condition to realize thermal rectification by either tuning QD levels or dot-lead couplings is numerically verified. We find that one can improve the thermal rectification effect by increasing electron-phonon coupling or reducing interdot coupling, while the electronic heat current is reduced.

## APPENDIX: HEAT CURRENT AND DYSON EQUATION IN TIME DOMAIN

One can define the following contour ordered Green's functions:

$$\widetilde{G}_{1,kL}(\tau_1,\tau_2) = -i\langle \mathcal{T}_C c_{kL}^\dagger(\tau_2) X_1(\tau_2) d_1(\tau_1) \rangle, \quad (A1)$$

$$\widetilde{G}_{2,kR}(\tau_1,\tau_2) = -i\langle \mathcal{T}_C c_{kR}^\dagger(\tau_2) X_2(\tau_2) d_2(\tau_1) \rangle, \quad (A2)$$

where $\mathcal{T}_C$ is the time ordering operator in the Keldsyh contour. From now on, the time on the contour is denoted using Greek letters, and real time using Latin letters. This implies that $\widetilde{G}_{1,kL}(\tau_1,\tau_2)$ and $\widetilde{G}_{2,kR}(\tau_1,\tau_2)$ are two-by-two matrices with their entries to be $\widetilde{G}_{1,kL}^{ab}(t_1,t_2)$ and $\widetilde{G}_{2,kR}^{ab}(t_1,t_2)$, respectively. Here $a,b = +,-$ denote the different branches of the contour. The lesser and greater Green's functions defined in Eq. (A1)

read, respectively, as

$$\widetilde{G}_{1,kL}^{+-}(t_1,t_2) = -i\langle c_{kL}^\dagger(t_2)X_1(t_2)d_1(t_1)\rangle, \quad (A3)$$

$$\widetilde{G}_{1,kL}^{-+}(t_1,t_2) = -i\langle d_1^\dagger(t_1)X_1^\dagger(t_2)c_{kL}(t_2)\rangle. \quad (A4)$$

Then heat current is given by

$$I_h(t) = \sum_k \epsilon_{kL} t_{kL} [\widetilde{G}_{1,kL}^{-+}(t,t) - \widetilde{G}_{1,kL}^{+-}(t,t)]. \quad (A5)$$

Having defined the Green's functions and heat current carried by electrons, we next employ equation of motion and the DTA to get the final heat current expression in terms of Fermi distribution functions and transmission coefficient function. The equation of motion of the three point Green function on the contour $\langle\mathcal{T}_C c_{kL}^\dagger(\tau_2)X_1(\tau')d_1(\tau_1)\rangle$ is

$$\left(i\frac{\partial}{\partial\tau_2} - \epsilon_{kL}\right)\langle\mathcal{T}_C c_{kL}^\dagger(\tau_2)X_1(\tau')d_1(\tau_1)\rangle$$
$$= t_{kL}^*\langle\mathcal{T}_C d_1^\dagger(\tau_2)X_1^\dagger(\tau_2)X_1(\tau')d_1(\tau_1)\rangle. \quad (A6)$$

The differential form could be written in an integral form [55] as

$$\langle\mathcal{T}_C c_{kL}^\dagger(\tau_2)X_1(\tau')d_1(\tau_1)\rangle$$
$$= \int_C d\tau \langle\mathcal{T}_C d_1^\dagger(\tau)X_1^\dagger(\tau)X_1(\tau')d_1(\tau_1)\rangle t_{kL}^* g_{kL}(\tau,\tau_2), \quad (A7)$$

where $g_{kL}(\tau,\tau_2)$ is the free electronic Green's function of the state $k$ in the left lead. One can define the DQD Green's function on the Keldysh contour as

$$G_{\nu\nu'}(\tau_1,\tau_2) = -i\langle\mathcal{T}_C d_{\nu'}^\dagger(\tau_2)d_\nu(\tau_1)\rangle, \quad (A8)$$

with $\nu,\nu' = 1,2$ labeling quantum dots.

The electron-phonon interaction is usually treated perturbatively for weak electron-phonon coupling [57]. However, in the strong electron-phonon coupling regime, the traditional perturbation technique fails and a nonperturbative approximation is needed. With the strong electron-phonon coupling and weak lead-dot coupling, the lifetime of the electronic states in DQD is much larger than that in the leads, DTA is suitable and can cope with the pathological features of the single particle approximation at low frequencies and polaron tunneling approximation at high frequencies [43]. Under DTA, one has the decoupling [43]

$$\langle\mathcal{T}_C d_1^\dagger(\tau)X_1^\dagger(\tau)X_1(\tau')d_1(\tau_1)\rangle$$
$$\simeq \langle\mathcal{T}_C X_1^\dagger(\tau)X_1(\tau')\rangle\langle\mathcal{T}_C d_1^\dagger(\tau)d_1(\tau_1)\rangle$$
$$= i\Lambda_1(\tau',\tau)G_{11}(\tau_1,\tau), \quad (A9)$$

and similarly

$$\langle\mathcal{T}_C d_2^\dagger(\tau)X_2^\dagger(\tau)X_2(\tau')d_2(\tau_1)\rangle = i\Lambda_2(\tau',\tau)G_{22}(\tau_1,\tau), \quad (A10)$$

with $\Lambda_\nu(\tau',\tau) = \langle\mathcal{T}_C X_\nu^\dagger(\tau)X_\nu(\tau')\rangle$ being the phonon cloud propagator. From Eqs. (A1), (A7), and (A9), we have

$$\widetilde{G}_{1,kL}(\tau_1,\tau_2)t_{kL} = \int_C d\tau G_{11}(\tau_1,\tau)t_{kL}^* g_{kL}(\tau,\tau_2)t_{kL}\Lambda_1(\tau_2,\tau). \quad (A11)$$

The above equation is expressed in Keldysh space and subscript "$C$" denotes the time integration in Keldysh contour. From Eqs. (A5) and (A11), heat current can be expressed as [53]

$$I_h = \int dt' [G_{11}^{+-}(t,t')\check{\Sigma}_{dL}^{-+}(t',t) - G_{11}^{-+}(t,t')\check{\Sigma}_{dL}^{+-}(t',t)], \quad (A12)$$

where

$$\check{\Sigma}_{dL}^{+-}(t',t) = -\Lambda_L^{+-}(t'-t)\sum_k \epsilon_{kL}t_{kL}^* g_{kL}^{+-}(t'-t)t_{kL} \quad (A13)$$

and similarly for $\check{\Sigma}_{dR}^{-+}(t',t)$.

For convenience, we use the lead index $\alpha$ instead of $\nu$ as the subindex for the phonon cloud operator so that $\Lambda_L(\tau_1,\tau_2) \equiv \Lambda_1(\tau_1,\tau_2)$ and $\Lambda_R(\tau_1,\tau_2) \equiv \Lambda_2^{ab}(\tau_1,\tau_2)$. Performing the summation over states $k$ in Eq. (A11), we obtain

$$\sum_k \widetilde{G}_{1,kL}(\tau_1,\tau_2)t_{kL} = \int_C d\tau G_{11}(\tau_1,\tau)\Sigma_L(\tau,\tau_2)\Lambda_L(\tau_2,\tau), \quad (A14)$$

where the self-energy is expressed as

$$\Sigma_L(\tau,\tau_2) = \sum_k t_{kL}^* g_{kL}(\tau,\tau_2)t_{kL}, \quad (A15)$$

with the Keldysh components

$$\Sigma_L^{ab}(t,t_2) = ab\sum_k t_{kL}^* g_{kL}^{ab}(t,t_2)t_{kL}. \quad (A16)$$

A similar expression for $\sum_k \widetilde{G}_{2,kR}(\tau_1,\tau_2)t_{kR}$ can be obtained as well. The self-energies dressed by the phonon cloud propagator under the DTA are then expressed as

$$\Sigma_{d\alpha}^{ab}(t_1,t_2) = \Sigma_\alpha^{ab}(t_1,t_2)\Lambda_\alpha^{ab}(t_1,t_2). \quad (A17)$$

The lesser and greater phonon cloud operator $\Lambda_\alpha^{ab}(t_1,t_2)$ are given by [35]

$$\Lambda_\alpha^{+-}(t_1,t_2) = [\Lambda_\alpha^{-+}(t_1,t_2)]^* = \sum_{m=-\infty}^\infty A_{\alpha m}e^{im\omega_0(t_1-t_2)}, \quad (A18)$$

with

$$A_{\alpha m} = e^{-g^2(2n_\alpha+1)}e^{m\beta_\alpha\omega_0/2}I_m(2g^2\sqrt{n_\alpha(1+n_\alpha)}), \quad (A19)$$

$I_m$ is the modified Bessel function of the first kind, and the Bose factor $n_\alpha = 1/(e^{\beta_\alpha\omega_0} - 1), \beta_\alpha = 1/k_B T_\alpha$. The remaining time-ordered and anti-time-ordered components could be calculated through the relations

$$\Lambda_\alpha^{++}(t_1,t_2) = \theta(t_1-t_2)\Lambda_\alpha^{-+}(t_1,t_2) + \theta(t_2-t_1)\Lambda_\alpha^{+-}(t_1,t_2),$$
$$\Lambda_\alpha^{--}(t_1,t_2) = \theta(t_2-t_1)\Lambda_\alpha^{-+}(t_1,t_2) + \theta(t_1-t_2)\Lambda_\alpha^{+-}(t_1,t_2). \quad (A20)$$

Taking the time derivative of the DQD NEGF $G_{\nu\nu'}(\tau_1,\tau_2)$ in Eq. (A8) [55] can give us the contour ordered Dyson equation of the system

$$\mathbf{G}(\tau_1,\tau_2) = \mathbf{g}(\tau_1,\tau_2) + \iint_C d\tau d\tau'\mathbf{g}(\tau_1,\tau)$$
$$\times [\Sigma_d(\tau,\tau') + \mathbf{t}\delta(\tau-\tau')]\mathbf{G}(\tau',\tau_2), \quad (A21)$$

with

$$\mathbf{G} = \begin{pmatrix} G_{11} & G_{12} \\ G_{21} & G_{22} \end{pmatrix}, \quad \mathbf{g} = \begin{pmatrix} g_1 & \\ & g_2 \end{pmatrix}, \quad \Sigma_d = \begin{pmatrix} \Sigma_{dL} & \\ & \Sigma_{dR} \end{pmatrix}, \quad \mathbf{t} = \begin{pmatrix} & t_{12} \\ t_{21} & \end{pmatrix}.$$

where $g_\nu$ is the free DQD Green's function of site $\nu$ without coupling to the leads.

---

[1] N. Li, J. Ren, L. Wang, G. Zhang, P. Häggi, and B. Li, Rev. Mod. Phys. **84**, 1045 (2012).

[2] D. G. Cahill, P. V. Braun, G. Chen, D. R. Clarke, S. Fan, K. E. Goodson, P. Keblinski, W. P. King, G. D. Mahan, A. Majumdar, H. J. Maris, S. R. Phillpot, E. Pop, and L. Shi, Appl. Phys. Rev. **1**, 011305 (2014).

[3] B. Sothmann, R. Sánchez, and A. N. Jordan, Nanotechnology **26**, 032001 (2015).

[4] R. Scheibner, M. König, D. Reuter, A. D. Wieck, C. Gould, H. Buhmann, and L. W. Molenkamp, New J. Phys. **10**, 083016 (2008).

[5] J. Ren and J.-X. Zhu, Phys. Rev. B **88**, 094427 (2013).

[6] J. Ren, Phys. Rev. B **88**, 220406(R) (2013).

[7] G. Tang, X. Chen, J. Ren, and J. Wang, Phys. Rev. B **97**, 081407(R) (2018).

[8] J. Ren and J.-X. Zhu, Phys. Rev. B **87**, 165121 (2013).

[9] J. Ren and J.-X. Zhu, Phys. Rev. B **89**, 064512 (2014).

[10] M. J. Martínez-Pérez, A. Fornieri, and F. Giazotto, Nat. Nanotechnol. **10**, 303 (2015).

[11] A. Fornieri, M. J. Martínez-Perez, and F. Giazotto, AIP Adv. **5**, 053301 (2015).

[12] Z. Chen, C. Wong, S. Lubner, S. Yee, J. Miller, W. Jang, C. Hardin, A. Fong, J. E. Garay, and C. Dames, Nat. Commun. **5**, 5446 (2014).

[13] G. Wu and B. Li, Phys. Rev. B **76**, 085424 (2007).

[14] N. Yang, G. Zhang, and B. Li, Appl. Phys. Lett. **95**, 033107 (2009).

[15] D. Sawaki, W. Kobayashi, Y. Moritomo, and I. Terasaki, Appl. Phys. Lett. **98**, 081915 (2011).

[16] X. Yang, D. Yu, and B. Cao, ACS Appl. Mater. Interfaces **9**, 24078 (2017).

[17] L.-A. Wu, C. X. Yu, and D. Segal, Phys. Rev. E **80**, 041103 (2009).

[18] L.-A. Wu and D. Segal, Phys. Rev. Lett. **102**, 095503 (2009).

[19] L. Zhang, Z. Yu, F. Xu, and J. Wang, Carbon **126**, 183 (2018).

[20] X. Chen, L. Zhang, and H. Guo, Phys. Rev. B **92**, 155427 (2015).

[21] Z. Yu, L. Zhang, Y. Xing, and J. Wang, Phys. Rev. B **90**, 115428 (2014).

[22] A. M.-Vicioso, C. López-Jurado, M. Ruiz-Garcia, and R. Sánchez, arXiv:1803.04073.

[23] D. M. T. Kuo and Y.-C. Chang, Nano. Res. Lett. **7**, 257 (2012).

[24] P. Thiessen, E. Díaz, R. A. Römer, and F. Domínguez-Adame, Phys. Rev. B **95**, 195431 (2017).

[25] C. R. Otey, W. T. Lau, and S. Fan, Phys. Rev. Lett. **104**, 154301 (2010).

[26] B. Li, L. Wang, and G. Casati, Phys. Rev. Lett. **93**, 184301 (2004).

[27] G. Schaller, G. G. Giusteri, and G. L. Celardo, Phys. Rev. E **94**, 032135 (2016).

[28] B. Liang, B. Yuan, and J.-c. Cheng, Phys. Rev. Lett **103**, 104301 (2009).

[29] N. Boechler, G. Theocharis, and C. Daraio, Nat. Mater. **10**, 665 (2011).

[30] D. Segal and A. Nitzan, Phys. Rev. Lett **94**, 034301 (2005).

[31] J. Reichert, R. Ochs, D. Beckmann, H. B. Weber, M. Mayor, and H. v. Löhneysen, Phys. Rev. Lett. **88**, 176804 (2002).

[32] W. Liang, M. Shores, M. Bockrath, J. Long, and H. Park, Nature (London) **417**, 725 (2002).

[33] S. Sapmaz, P. Jarillo-Herrero, Y. M. Blanter, C. Dekker, and H. S. J. van der Zant, Phys. Rev. Lett. **96**, 026801 (2006).

[34] T. Holstein, Ann. Phys. (NY) **8**, 343 (1959).

[35] G. D. Mahan, *Many-Particle Physics*, 3rd ed. (Kluwer Academic, Dordrecht, 2000).

[36] M. Poot and H. S. J. van der Zant, Phys. Rep. **511**, 273 (2012).

[37] A. Benyamini, A. Hamo, S. V. Kusminskiy, F. von Oppen, and S. Ilani, Nat. Phys. **10**, 151 (2014).

[38] F. Ortmann, F. Bechstedt, and K. Hannewald, Phys. Rev. B **79**, 235206 (2009).

[39] F. Ortmann and S. Roche, Phys. Rev. B **84**, 180302 (2011).

[40] S. Walter, B. Trauzettel, and T. L. Schmidt, Phys. Rev. B **88**, 195425 (2013).

[41] J. K. Sowa, J. A. Mol, G. A. D. Briggs, and E. M. Gauger, Phys. Rev. B **95**, 085423 (2017).

[42] B. Dong, G. H. Ding, and X. L. Lei, Phys. Rev. B **88**, 075414 (2013).

[43] R. Seoane Souto, A. Levy Yeyati, A. Martín-Rodero, and R. C. Monreal, Phys. Rev. B **89**, 085412 (2014).

[44] B. Dong, G. H. Ding, and X. L. Lei, Phys. Rev. B **95**, 035409 (2017).

[45] J. Koch and F. von Oppen, Phys. Rev. Lett. **94**, 206804 (2005).

[46] J. Koch, F. von Oppen, and A. V. Andreev, Phys. Rev. B **74**, 205438 (2006).

[47] P. Haughian, S. Walter, A. Nunnenkamp, and T. L. Schmidt, Phys. Rev. B **94**, 205412 (2016).

[48] T. L. Schmidt and A. Komnik, Phys. Rev. B **80**, 041307(R) (2009).

[49] G. A. Kaat and K. Flensberg, Phys. Rev. B **71**, 155408 (2005).

[50] K. Ono, D. G. Austing, Y. Tokura, and S. Tarucha, Science **297**, 1313 (2002).

[51] D. Malz and A. Nunnenkamp, Phys. Rev. B **97**, 165308 (2018).

[52] L. V. Keldysh, Zh. Eksp. Teor. Fiz. **47**, 1515 (1964) [Sov. Phys. JETP **20**, 1018 (1965)].

[53] Z. Yu, G.-M. Tang, and J. Wang, Phys. Rev. B **93**, 195419 (2016).

[54] G. Tang, Z. Yu, and J. Wang, New J. Phys. **19**, 083007 (2017).

[55] H. Haug and A.-P. Jauho, *Quantum Kinetics in Transport and Optics of Semiconductors* (Springer, Berlin, 1998).

[56] A. Kamenev, *Field Theory of Non-Equilibrium Systems* (Cambridge University Press, Cambridge, 2011).

[57] A. Ueda and M. Eto, Phys. Rev. B **73**, 235353 (2006).